Annals of the University of Craiova, Electrical Engineering series, No. 46, Issue 1, 2022; ISSN 1842-4805 eISSN 2971-9852

DOI: 10.52846/AUCEE.2022.06

Exhaustive Optimization Method Applied on Electromagnetic Device

Alin-Iulian Dolan
University of Craiova, Faculty of Electrical Engineering, Craiova, Romania, adolan@elth.ucv.ro

***Abstract* –This paper presents the application of an exhaustive optimization method based on the design of experiments (DOE) and the finite element method (FEM), with the aim of improving the actuation force developed by a DC electromagnet. The optimization of this device has been the subject of several previous works, allowing comparisons between the optimization methods applied in terms of the obtained precision and the workload. According to previous studies, two geometric parameters (the angle ratio of the support tip and the coil shape ratio) are very influential on the force developed at the maximum air gap. Thus, the exhaustive optimization method took into account these two parameters for its maximization, having as constraints the maintenance of the global dimensions of the device (external radius, the height of carcass, height of the plunger with support) and of the cross-section of the winding. The optimization algorithm used the results of 2-D FEM numerical experiments carried out with the FEMM program in combination with the LUA language and is based on the response surface methodology (RSM) and analysis of variance (ANOVA). Second-order polynomial models of the objective function were calculated using full factorial designs with three levels per factor. After three iterations, a very good result was obtained, comparable to those obtained by other methods, but with a significant cost in terms of workload, the optimum obtained being a global one.**

Cuvinte cheie: *optimizare, proiectarea experimentelor, metodologia suprafeţelor de răspuns, analiză dispersională, metoda elementelor finite 2-D.*

Keywords: *optimization, DOE, RSM, ANOVA, 2-D FEM.*

I. INTRODUCTION

Finite element modeling (FEM) techniques successfully replace real experiments, making significant contributions to solving problems in electromagnetism, especially when combined with the design of experiments (DOE) technique [1], [2].

The electromagnet is an electrical equipment designed to transform electrical energy into mechanical energy, developing a force that acts on a moving armature. It is often found in switches, relays and valves due to its simplicity of construction, reliability and low cost. Many scientific works have presented studies on improving the performance in terms of the force developed, based on the analysis of the magnetic field through FEM and different optimization techniques, aiming at reducing the reluctance of the magnetic circuit and increasing the magnetic flux density in the air-gap [3] – [27].

In [3] was presenteda 3-D axial-symmetric finite element method analysis combined with the quadratic sequential programming (SQP) to optimize of the geometric shape of the plunger of a DC actuator for increasing the static thrust characteristic. In [4] was created a 3-D shape optimization algorithm combining the geometric parameterization of the design surface with B-spline technique and design sensitivity analysis to optimize the pole face of an electromagnet, obtaining a uniform distribution of magnetic field on the target region from the air gap. In [5] was used the level set based topology optimization to maximize the actuating force, subject to limited usage of ferromagnetic material.

The work [6] presented structural topology optimization of an electro/permanent magnet linear actuator. The used tools are Maxwell Stress Tensor (MST) approach coupled with FEM for magnetic force computation, the adjoint method for the optimization sensitivity analysis and the sequential linear programming (SLP) for solving the optimization problem.

The response surface technology (RSM), DOE, FEM and SLP were combined in [7] to optimize a linear actuator with permanent magnet for driving a needle in a knitting machine.

In [8] was proposed an optimized topology of a solenoid with unified coil that operates valves in aircraft engine under harsh environmental conditions and high endurance requirements. The solution aims at developing higher force for the constrained size or the same force for less size and weight of the solenoid. In [9] was presented an optimization technique for average electromagnetic force of an actuator.

In [10] was performed a shape optimization of the plunger of an electromagnetic actuator in order to obtain linear static characteristic. Using suitable genetic algorithms, it is proven that the properly shaped plunger can strongly influence its static characteristic. In [11] was discussed a technique of optimal design for actuators with permanent magnet for the class of medium voltage of vacuum circuit breakers. Using the RSM technique combined with FEM are obtained improvement of dynamic characteristics and minimization of permanent magnet weight.

The influence of the plunger shape on the developed force of a DC electromagnetic actuator and on its time response were presented in [12]. The optimization of the plunger shape was made using a 2-D axial-symmetric model by genetic algorithm and the analysis of magnetic subsystem of actuator was performed by FEM implemented with ANSYS Electronics software.

The paper [13] presented the maximization of the magnetic force of an actuator which tends to be highly dependent on the geometry around air gap. Using the approach of MST through the isogeometric analysis for force computation, the optimization problem is solved using a gradient-based algorithm of modified method of feasible directions. The research in [14] brought a new level-set-based topology optimization method for magnetic actuator design using two remeshing techniques: the modified adaptive mesh method and the extended finite-element method (XFEM). The tools were used to maximize the magnetic force under the constraint of the ferromagnetic material volume.

In [15] was presented an optimization technique based on a parametric and topology optimization method for determination of the optimized configuration of a permanent magnet actuator (PMA), maximizing the magnetic force subject to an unchangeable volume fraction constraint for each material.

As one of the branches of DOE, the RSM was used in combination with FEM in [16] to make a screening of significant parameters of an electrical motor in order to optimize its performances. The same techniques were applied in [17] to improve an electromagnet in magnetic levitation system based on many design variables.

The maximization of the force developed by an electromagnetic actuator was often an appropriate case study to prove and validate different optimization techniques. The SQP method was applied in [18] to a linear actuator after validation of a shape sensitivity analysis of magnetic forces by the MST approach and FEM. Improvement of static characteristic of an electromagnet was made in [19] by the same tool.

In [20] was successfully performed the maximization of the clamping force of an electromagnetic linear actuator with divided coil excitation by using RSM.

Coupling the RSM with 2-D FEM was applied in [21] to develop mathematical relationships between input design parameters and output performance parameters of a tubular permanent magnet brushless linear motor with Halbach magnet array, in order to optimize its efficiency, specific power and cost.

In recent papers [22], [23] were presented optimal solutions of a DC electromagnet (Fig. 1) providing a maximi-zed static force characteristic [22], respectively, a maximum electromagnetic force related to the largest air-gap (actuating force) [23], preserving the global dimensions of the device and the cross-section of the winding. The used tools were DOE and 2-D FEM.

Two parameters were taken into account to maximize the static characteristic in [22] and three parameters were used to maximize the acting force in [23].

The work [25] carried out previous analyses proposing an optimal shape of the same DC device, subject to the same constraints, expanding research on a fourth geometrical parameter. To justify the use of these four parameters in the optimization process, was performed a screening of DC electromagnet that has proved that all the four parameter have best influence on the static force characteristic, with 99% confidence.

These are the angle ratio support tip k_β, the coil shape ratio k_b, the support thickness ratio k_{a1}, and the support height ratio k_v:

$$k_\beta = \frac{\beta}{\beta_1} \in [0.67 \div 1.33] \tag{1}$$

$$k_b = \frac{h_b}{g_b} \in [6 \div 8] \tag{2}$$

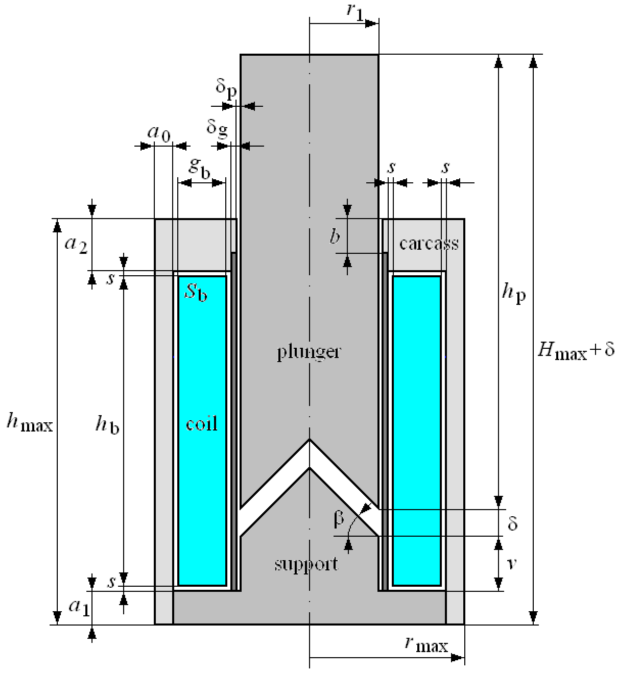

Fig. 1. Geometry of DC electromagnet [22].

$$k_{a1} = \frac{a_1}{a} \in [0.9 \div 1.1] \tag{3}$$

$$k_v = \frac{v}{h_b} \in [0.15 \div 0.20] \tag{4}$$

where $\beta_1 = 45°$ is initial value of the angle β and $a = 14.90$ mm is the initial value of support thickness.

The studies continued in the work [26] with the extension to six of the number of parameters taken into account to the maximization of the actuating force, using the optimization method based on zooms in experimental domain.

The design methodology [24] indicates the initial values of geometrical parameters with their ranges and Table I summarizes them [22]. The air-gap varies in range $\delta = [1 \div 41]$ mm, the winding has $N = 1269$ turns of standard diameter $d = 0.8$ mm and the rated voltage is $U_r = 110$ V DC. For $\delta = [10 \div 41]$ mm and $\delta = [1 \div 10]$ mm the currents are $I_1 = 12.92$ A, respectively, $I_2 = 6.90$ A, depending on absence or presence of an economy resistor.

In Fig. 2 are done the magnetization curves of the core of steel (plunger with support) and of the carcass of cast iron [22].

All the optimization methods used in works [22], [23], [23], [26] are methods that allow the determination of an local extremum, which can be the global one if the initial point with which the algorithm starts is placed in its vicinity.

The present paper aims to verify whether in the optimization problem having the actuation force as objective function, there are also local maximums. In other words, the aim is to verify the unimodality of the objective function.

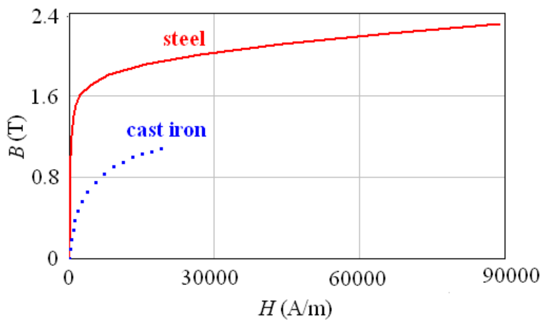

Fig. 2. Magnetization curves for core (plunger with support) (steel) and for carcass (cast iron) [22].

TABLE I.
GEOMETRICAL PARAMETERS OF DC ELECTROMAGNET [22]

r_1 (mm)	29.80	g_b (mm)	19.83	b=0.671a_2 (mm)	10.00
β_1 (°)	45.00	h_b (mm)	138.90	δ_p (mm)	1.00
a_1 (mm)	14.90	s (mm)	2.00	δ_g (mm)	2.00
a_2 (mm)	14.90	v (mm)	24.29	S_b=$g_b h_b$ (mm^2)	2752.27
a_0 (mm)	9.07	h_p (mm)	192.00		

For this was applied an exhaustive optimization method [2] based on the same numerical instruments, taking into account the first two geometric parameters, proven very influential [25], slightly expanding the variation range of the first:

$$k_\beta = \frac{\beta}{\beta_1} \in [0.467 \div 1.533] \qquad (5)$$

$$k_b = \frac{h_b}{g_b} \in [6 \div 8] \qquad (6)$$

This method has been used successfully to optimize a Superconducting Magnetic Energy Storage (SMES) device [27].

II. Exhaustive Optimisation Methods Based on Response Surface Methodology

The exhaustive optimization methods proceed to a complete and systematic analysis of the feasible domain by realization of designs of experiments put side by side or stacked [2]. The applied algorithm uses the RSM and zoom operations.

The response surface methodology (RSM) is a useful technique for modeling and analysis of the response of a system influenced by a set of independent factors. The DOE is essentially based on the creation and exploitation of the models of the response consisting of analytical relationship describing the variations of the response versus to the variation of the factors [1]. Usually, the RSM pro-blems use polynomial models of first- or second-order derived as results of a series of experiments with different values for the factors.

For a set of k factors, the model function (regression) Y_{mod} approximates the value of response Y for any combination of the factors. The second-order models use qua-dratic terms and p = 6 coefficients

$$Y_{\text{mod}}(\boldsymbol{x}) = f(\boldsymbol{x}) \cdot \boldsymbol{\beta} \qquad \boldsymbol{x} = (x_1 \ldots x_k)^{\mathrm{T}} \qquad (7)$$

$$f(\boldsymbol{x}) = (1\ x\ y\ xy\ x^2\ y^2),\ \boldsymbol{\beta} = (b_0\ b_1\ b_2\ b_{12}\ b_{11}\ b_{22})^{\mathrm{T}} \quad (8)$$

A. Estimation of Coefficients of Polynomial Models

For N experiments and 2 factors, the value of the model function in any experience point $\mathrm{P}_i\ (\boldsymbol{x}_i) = \mathrm{P}_i\ (x_i, y_i)$ is

$$Y_{\text{mod}}(\boldsymbol{x}_i) = f(\boldsymbol{x}_i) \cdot \boldsymbol{\beta}, \quad 1 \le i \le N \qquad (9)$$

In most common situations $N > p$ and there is enough information in the experimental data to estimate a unique value for $\boldsymbol{\beta}$ such that the model best fits the response. It commits an adjustment error in each of these points. So there is an error vector $\boldsymbol{\varepsilon}$ (residue) nonzero. The coefficients can be estimated by minimization of the vector $\boldsymbol{\varepsilon}$ by the least squares criterion. The matrix-form relationship linking the response and the model function based on the estimation vector $\hat{\boldsymbol{\beta}}$ is

$$\boldsymbol{Y} = \left(Y(\boldsymbol{x}_1) \ldots Y(\boldsymbol{x}_N)\right)^{\mathrm{T}} = \left(f(\boldsymbol{x}_1) \ldots f(\boldsymbol{x}_N)\right)^{\mathrm{T}} \cdot \hat{\boldsymbol{\beta}} + \boldsymbol{\varepsilon} \quad (10)$$

$$\sum_{i=1}^{N} \varepsilon_i^{\,2} = \sum_{i=1}^{N} \left(Y(\boldsymbol{x}_i) - Y_{\text{mod}}(\boldsymbol{x}_i)\right)^2 \rightarrow \min \qquad (11)$$

B. Analysis of Variance (ANOVA) of the Model and Adjusting Coefficients

The ANOVA can be used to test the validity of the model function based on the relationship [2]

$$\boldsymbol{Y}^{\mathrm{T}} \cdot \boldsymbol{Y} = \boldsymbol{Y}_{mod}^{\ \ \mathrm{T}} \cdot \boldsymbol{Y}_{mod} + \boldsymbol{\varepsilon}^{\mathrm{T}} \cdot \boldsymbol{\varepsilon} \quad \Leftrightarrow \quad SST = SSR + SSE \quad (12)$$

The left terms, called the total sum of the squares (SST) is composed of the sum of squares due to regression (SSR) and of the sum of errors squares (SSE). The variances (the mean squares) of the responses, regression and residues are deducted dividing the sums of squares by the corres-ponding degrees of freedom (DOF). Suppressing the constant terms corresponding to coefficient b_0, the DOFs decrease by 1. Thus

$$MST_{-0} = \frac{SST}{N-1} \quad MSR_{-0} = \frac{SSR}{p-1} \quad MSE = \frac{SSE}{N-p} \quad (13)$$

The Fisher-Snedecor test is performed calculating ratio

$$F_{\text{obs}} = \frac{MSR_{-0}}{MSE} \qquad (14)$$

The MSR_{-0} can be considered of the same order as MSE if the ratio F_{obs} is less than a statistical threshold. The null hypothesis H_0 means that $\boldsymbol{\beta} = \boldsymbol{0}$. Under this assumption, F_{obs} is an observed value of a variable F of Fisher-Snedecor type, with p (or $p-1$) and $(N-p)$ DOFs.

The hypothesis H_0 must be rejected at level λ when the probability $P(F \ge F_{\text{obs}}) \le \lambda$.

The quality of a model can be evaluated by some adjustments coefficients:

- Coefficient of determination (R^2) is the ratio of the variance explained by the regression by the variance of responses, both corrected by the average value $\bar{Y}$

$$R^2 = \frac{\boldsymbol{Y}_{mod}^{\ \ \mathrm{T}} \cdot \boldsymbol{Y}_{mod} - \bar{\boldsymbol{Y}}^{\mathrm{T}} \cdot \bar{\boldsymbol{Y}}}{\boldsymbol{Y}^{\mathrm{T}} \cdot \boldsymbol{Y} - \bar{\boldsymbol{Y}}^{\mathrm{T}} \cdot \bar{\boldsymbol{Y}}} = \frac{SSR_{-\mathrm{m}}}{SST_{-\mathrm{m}}} = \frac{SST_{-\mathrm{m}} - SSE_{-\mathrm{m}}}{SST_{-\mathrm{m}}} \quad (15)$$

- Adjusted coefficient of determination ($R_a^{\ 2}$) is defined in relation to corresponding DOFs

$$R_a^{\ 2} = \left(\frac{SST_{-\mathrm{m}}}{N-1} - \frac{SSE_{-\mathrm{m}}}{N-p}\right) \Big/ \left(\frac{SST_{-\mathrm{m}}}{N-1}\right) \qquad (16)$$

- Rate of coefficient of variation by difference between the extreme values of the responses on the current subdomain

$$\Delta = \frac{\hat{\sigma}}{\Delta y} = \frac{\sqrt{SSE}}{\Delta y} \tag{17}$$

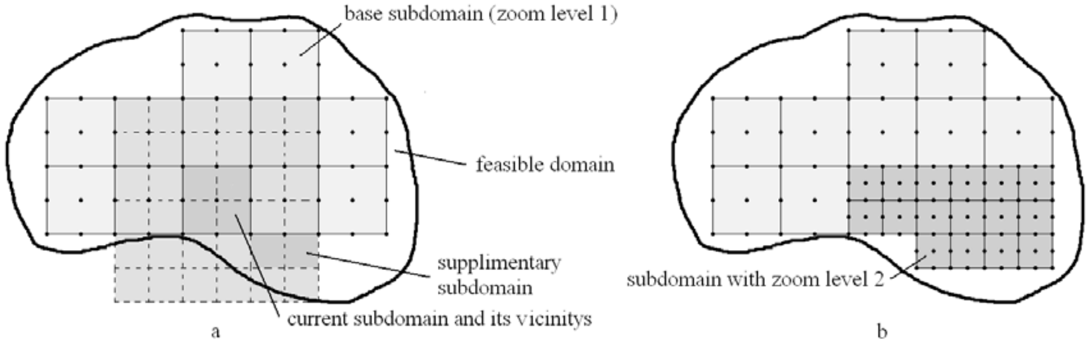

Fig. 3. Description of the exhaustive optimization algorithm [27].

The goal of the exhaustive optimization method is to modeling the objective function by subdomains, performing on each of them a full factorial design with 3 levels per factor, in order to calculate a polynomial model of 2-nd order. If k is the number of factors, result 3^k experiments per subdomain.

The partitioning of study domain is made with an initial hyper-rectangular grid chosen by experimenter, covering the great part of feasible domain, such that exist at least two neighbor subdomains along each of the k dimensions (base subdomains) (Fig. 3a). The candidate points must not be excluded by the constraints on position.

Each analyzed hyper-rectangular subdomain (current subdomain) may be subject to constraints on reached value. Before performing all the 3^k experiments, is made a summary analysis of its 2^k corners: if none of them fulfills the constraints on reached value no longer performs the rest of $3^k - 2^k$ experiments and the next subdomain is analyzed. Otherwise, the rest of experiments are performed.

A calculated model is considered valid if its adjustment coefficients exceed the threshold indicated by experimenter ($R^2 \geq R^2_{\lim}$, $R_a^{\,2} \geq R_a^{\,2}{}_{\lim}$, $\hat{\sigma}/\Delta y \leq \Delta_{\lim}$, $P \geq P_{\lim}$). Otherwise, the current subdomain must be divided into 2^k subdomains where the same process is repeated.

The algorithm uses a parameter called maximum zoom level that defines the maximum number of scissions of the base subdomain plus 1.

By hypothesis, the base subdomain is realized with a unit level of zoom (Fig. 3a). This parameter allows setting the stop condition of the algorithm. The scission of a base subdomain generates 2^k subdomains with zoom level 2 (Fig. 3b).

The accuracy of the modeling can be set by the parameter called minimum zoom level that defines the minimum number of scissions to apply to the base subdomain.

For the boundary subdomains, a supplementary analysis of theirs vicinities can be useful for better covering of the feasible domain. So, if a boundary subdomain must be divided into 2^k parts, then the analysis is extended to the neighbour subdomains in order to find some parts of them (supplementary subdomains) which can complete the initial grid (Fig. 3a).

The algorithm is recursive. It calls itself either whether the minimum number of zooms is not reached or whether the maximum number of zooms is not reached, or whether none of the criteria of quality is fulfilled.

III. Optimization Problem and Its Solving

The optimization problem is the maximization of the electromagnetic force at δ = 41 mm, calling actuating force (F_a), which is set as objective function. This is a 2-D nonlinear optimization problem subject to four equality constraints consisting in preserving the global dimensions of the device (the external radius $r_{\max}$, the height of carcass $h_{\max}$, the height of plunger with support $H_{\max}$) and the coil cross section ($S_b = g_b \cdot h_b$). The complete form (P) of the optimization problem is

$$\mathrm{P}:\begin{cases}\min F_a(k_\beta, k_b, a_0, a_2, h_p, g_b)\\ k_{\beta\min} \leq k_\beta \leq k_{\beta\max}\\ k_{b\min} \leq k_b \leq k_{b\max}\\ g_r(k_b, k_{a1}, k_v) = 0\\ g_h(k_b, k_{a1}, k_v) = 0\\ g_H(k_b, k_{a1}, k_v) = 0\\ g_{Sb}(k_b, k_{a1}, k_v) = 0\end{cases} \tag{18}$$

$$g_r(k_b) = r_1 + \delta_p + \delta_g + 2s + g_b(k_b) + a_0(k_b) - r_{\max} \tag{19}$$

$$g_h(k_b, k_{a1}) = k_{a1}a + a_2(k_b, k_{a1}) + 2s + k_b \cdot g_b(k_b) - h_{\max} \tag{20}$$

$$g_H(k_b, k_{a1}, k_v) = h_p(k_b, k_{a1}, k_v) + k_v \cdot k_b \cdot g_b(k_b) + k_{a1} \cdot a - H_{\max} \tag{21}$$

$$g_{Sb}(k_b) = k_b \cdot \left[g_b(k_b)\right]^2 - S_b \tag{22}$$

where a = 14.90 mm, $r_{\max}$ = 65.70 mm, $h_{\max}$ = 172.60 mm, $H_{\max}$ = 231.19 mm, S_b = 2752.27 mm^2 are initial values resting constant.

The 2-D feasible domain is represented in Fig. 4, being a rectangular domain, in which there are only positional constraints, related to the parameters' limits.

For the zoom level ζ = 1, the feasible domain was partitioned into a number of 4 × 4 = 16 basic subdomains on which the ANOVA technique was applied, obtaining different response surfaces, whose quality was tested by calculating the four adjustment coefficients of P, R^2, $R_a^{\,2}$, Δ.

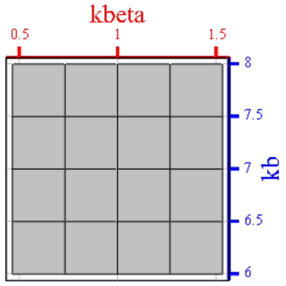

Fig. 4. The 2-D feasible domain and basic subdomains (ζ = 1).

Theirs chosen thresholds are established to be: P_{lim} = 0.99, $R^2{}_{\text{lim}}$ = 0.98, $R_a{}^2{}_{\text{lim}}$ = 0.95, Δ_{lim} = 0.08. The maximum zoom level was chosen to be ζ_{lim} = 3.

The differences between the values of the adjustment coefficients are represented chromatically in Fig 5, noting isolated areas with nuances much different from the majority, indicating the uncertainty subdomains of the local or global maxima. Subdomains of unsatisfactory quality (column no. 4) still require partitioning.

For the zoom level ζ = 1 the optimal value is obtained in the point P_1 having the coordinates k_β = 1.4000 and k_b = 6.5000, with value F_{a1} = 808.767 N, meaning a gain of 23.19%, comparatively with initial value F_a = 656.522 N. The point P_1 is visible in Fig. 9. In the subdomains in which the quality criteria are fulfilled was not performed the full factorial design and these appear not divided.

In Fig. 6 are represented the results obtained for ζ = 2, with optimal solution in the point P_2(1.4667, 6.6250), F_{a2} = 811.053N, gain 23.54% and in Fig. 7, the results for ζ = 3, with optimal solution in P_3(1.4333, 6.5625), F_{a3} = 813.583N, gain 23.92%.

These values are comparable with the previous ones.

Fig. 8 collects the results shown in Figs. 5-7, highlighting a single "island" of color much different from the rest, which indicates the presence of a single maximum, which proves the unimodality of the objective function up to this zoom level. The points P_2 and P_3 are visible in Fig. 10 and Fig. 11.

Two stopping criterions limit the number of iterations, when the accuracy is acceptable. Thus, the value computed is compared with initial one:

$$\varepsilon_1\,[\%] = \frac{F_a^{\,(t)} - F_{\text{a\_in}}}{F_{\text{a\_in}}} \cdot 100 \le \varepsilon_{1\max}\,[\%] \qquad (23)$$

or the value computed per iteration (t) is compared with the previous different one (s) ($1 \le s \le t-1$):

$$\varepsilon_2\,[\%] = \frac{F_a^{\,(t)} - F_a^{\,(s)}}{F_a^{\,(s)}} \cdot 100 \le \varepsilon_{2\max}\,[\%] \qquad (24)$$

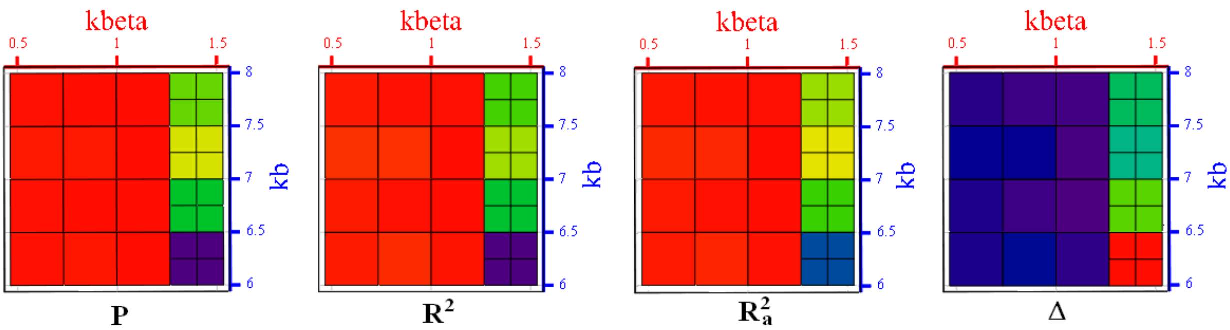

Fig. 5. The chromatic highlighting of the differences between the values of the adjustment coefficients on the basic subdomains (ζ = 1).

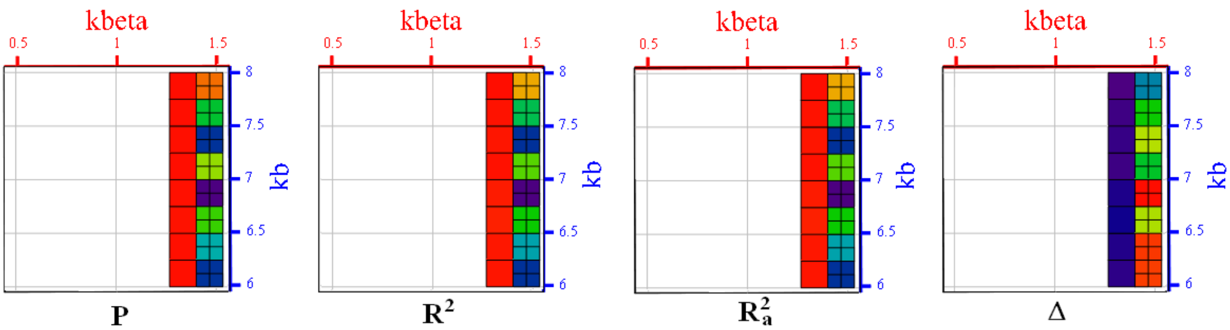

Fig. 6. The chromatic highlighting of the differences between the values of the adjustment coefficients on the subdomains with ζ = 2.

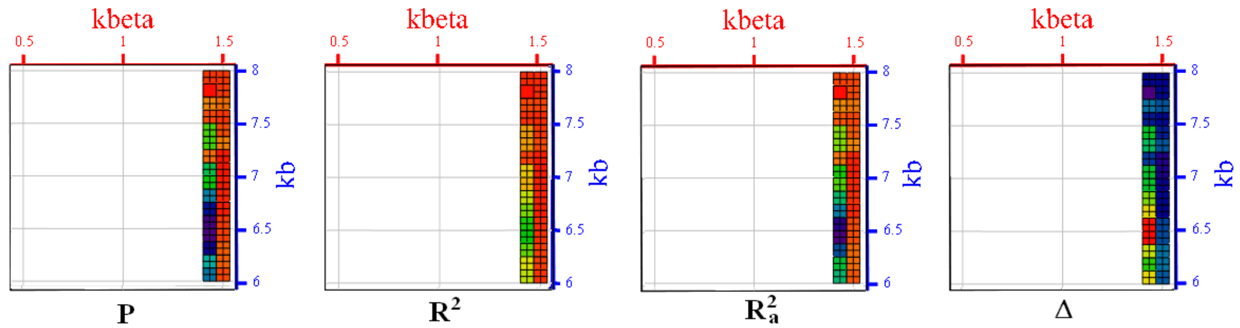

Fig. 7. The chromatic highlighting of the differences between the values of the adjustment coefficients on the subdomains with ζ = 3.

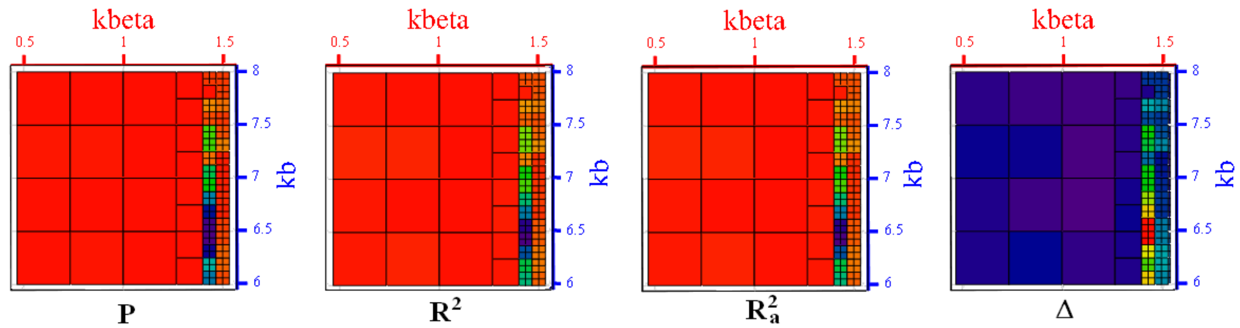

Fig. 8. The chromatic highlighting of the differences between the values of the adjustment coefficients on the analysed subdomains (ζ = 1, 2, 3).

The applied exhaustive optimization method requires a total of N = 577 numerical 2-D FEM experiments. More than half (324 experiments) can be recovered from previous iterations, resulting in a real number of 253 experiments.

In Table II are summarized the results of application of the optimization algorithm to the electromagnetic device along the three iterations, showing the variation of the design parameters, objective function, errors and main geometrical parameters.

Figure 12 presents on left and right sides the initial and the optimal geometrical shapes with the distributions of magnetic flux density obtained in FEMM software as axisymmetric solution.

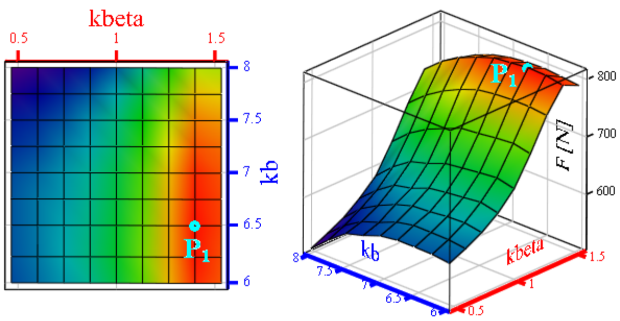

Fig. 9. The values of the objective function in the nodes of the partitioned basic subdomains and the optimal value for ζ = 1 (Point P_1).

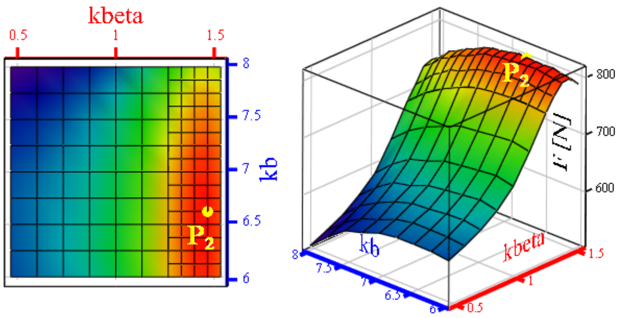

Fig. 10. The values of the objective function in the nodes of the partitioned basic subdomains and the optimal value for ζ = 2 (Point P_2).

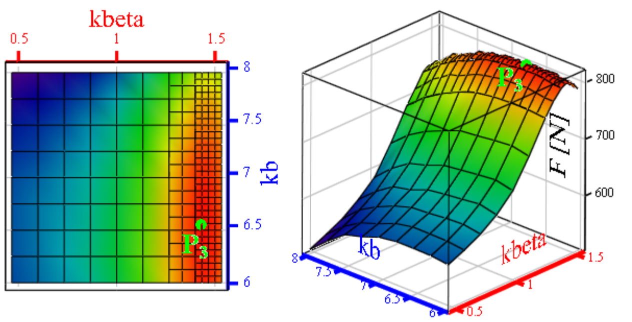

Fig. 11. The values of the objective function in the nodes of the partitioned basic subdomains and the optimal value for ζ = 3 (Point P_3).

TABLE II. QUANTITIES VARIATION DURING THE OPTIMIZATION PROCESS: DESIGN PARAMETERS, OBJECTIVE FUNCTION F_a, ERRORS AND MAIN GEOMETRICAL PARAMETERS

Iterations	N_{tot}	N_{rec}	k_β	k_b	F_a (N)	ε_1 (%)	ε_2 (%)	β (°)	g_b (mm)	h_b (mm)	a_0 (mm)	a_2 (mm)	v (mm)	h_p (mm)
Initial	1	-	1.0000	7.0000	656.522	-	-	45.00	19.83	138.80	9.07	14.90	24.29	192.00
1	144	64	1.4000	6.5000	808.767	23.19	23.19	63.00	20.58	133.75	8.32	19.95	23.41	192.89
2	144	86	1.4667	6.6250	811.053	23.54	0.28	66.00	20.38	135.03	8.52	18.67	23.63	192.66
3	288	174	1.4333	6.5625	813.583	23.92	0.31	64.50	20.48	134.39	8.42	19.31	23.52	192.77
Total	577	324												

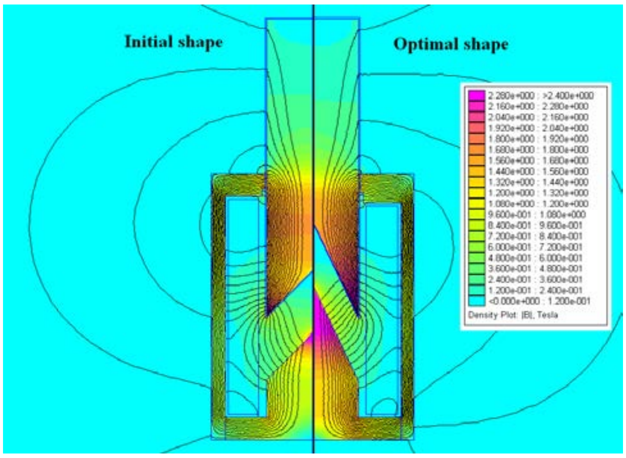

Fig. 12. Distribution of magnetic flux density for initial (left) and optimal (right) shapes (δ = 41 mm, FEMM, axisymmetric solution).

IV CONCLUSIONS

The paper presents the application of an exhaustive optimization method based on DOE and 2-D FEM, on a DC electromagnetic device. This was the subject of several previous works that investigated the improvement of its performances through methods of the same type, but capable of determining only a local optimum.

The optimization problem is nonlinear and it consists in maximization of the actuating force taking into account two geometric parameters (the angle ratio of the support tip and the coil shape ratio) subject to equality constraints which describe the preservation of the global dimensions of the device and of the cross-section of the winding.

The exhaustive optimization algorithm used the values of numerical simulation with FEMM software and it allowed the determination of the global optimum which corresponds to a gain in actuation force of 23.92%, from 656.522 N to 813.583N.

The result obtained in this paper is comparable to the previous ones, validating the old methods with a significant cost in the workload.

ACKNOWLEDGMENT

Source of research funding in this article: Research program of the Electrical Engineering Department financed by the University of Craiova.

Contribution of authors:

First author – 100%

Received on July 17, 2022

Editorial Approval on November 20, 2022

REFERENCES

[1] D. Montgomery, Design and analysis of experiment, 5-th Edition, Arizona State University, 2000.

[2] S. Vivier, “Strategies d’optimisation par la methode des plans d’experiences et applications aux dispositives electrotechniques modelise par elements finis,” Ph-D Thesis, Lille, 2002.

[3] S.-B. Yoon, J. Hur, Y.-D. Chun, and D.-S. Hyun, “Shape optimization of solenoid actuator using the finite element method and numerical optimization technique,” IEEE Transactions on Magnetics, Vol.33, No. 5, pp. 4140-4142, September, 1997.

[4] J.-S. Ryu, Y. Yao, C.-S. Koh,S. Yun, and D.-S. Kim, “Optimal Shape Design of 3-D Nonlinear Electromagnetic Devices Using Parameterized Design Sensitivity Analysis,” IEEE Transactions on Magnetics, Vol. 41, No. 5, pp.1792-1795, May, 2005.

[5] S.-I. Park, and S. Min, “Magnetic Actuator Design for Maximizing Force Using Level Set Based Topology Optimization,” IEEE Transactions on Magnetics, Vol. 45, No. 5, pp.2336-2339, May, 2009.

[6] J. Lee, E.-M. Dede, and T. Nomura, “Simultaneous Design Optimization of Permanent Magnet, Coils, and Ferromagnetic Material in Actuators,” IEEE Transactions on Magnetics, Vol. 47, No. 12, pp. 4712-4716, May, 2011.

[7] I. Yatchev, M. Rudnicki, K. Hinov, and V. Gueorgiev, “Optimization of a permanent magnet needle actuator,” COMPEL, Vol. 31, Issue 3, pp. 1018-1028, 2012.

[8] R. Narayanswamy, D.-P. Mahajan, and S. Bavisetti, “Unified Coil Solenoid Actuator for Aerospace Application,” Proceedings of IEEE Electrical Systems for Aircraft, Railway and Ship Propulsion, Bologna, October 16-18, pp. 1-5, 2012.

[9] S. Yong, J. Tong, S. Enze, and Y. Zaiming, “Analysis and optimization of static characteristics in overall operating conditions of electromagnetic actuator,” Research Journal of Applied Sciences, Engineering and Technology 7(8), pp. 1561-1567, 2014.

[10] F. Mach, I. Novy, P. Karban, and I. Dolezel, “Shape Optimization of Electromagnetic Actuators,” Proceedings of IEEE ELEKTRO, Bologna, May 19-20, pp. 595-598, 2014.

[11] H.-M. Ahn, T.-K. Chung, Y.-H. Oh, K.-D. Song, Y.-I. Kim, H.-R. Kho, M.-S. Choi, and S.-C. Hahn, “Optimal Design of Permanent Magnetic Actuator for Permanent Magnet Reduction and Dynamic Characteristic Improvement using Response Surface Methodology,” J. Electr. Eng. Technol.2015, 10(3): pp. 935-943, 2015.

[12] E. Plavec, and M. Vidović, “Genetic Algorithm Based Plunger Shape Optimization of DC Solenoid Electromagnetic Actuator,” Proceedings of 24th IEEE Telecommunications Forum (TELFOR), Belgrade, pp. 1-4, 2016.

[13] S.-W. Lee, J. Lee, and S. Cho, “Isogeometric Shape Optimization of Ferromagnetic Materials in Magnetic Actuators,” IEEE Transactions on Magnetics, Vol. 52, No. 2, pp. 1-8, February, 2016.

[14] S. Jeong, S. Lim, and S. Min, “Level-Set-Based Topology Optimization Using Remeshing Techniques for Magnetic Actuator Design,” IEEE Transactions on Magnetics, Vol. 52, No. 3, pp. 1-4, March, 2016.

[15] S. Lim, S. Jeong, and S. Min, “Multi-Component Layout Optimization Method for the Design of a Permanent Magnet Actuator,” IEEE Transactions on Magnetics, Vol. 52, No. 3, pp. 1-4, March, 2016.

[16] F. Gillon, and P. Brochet, “Screening and response surface method applied to the numerical optimization of electromagnetic devices,” IEEE Transaction on Magnetics, Vol. 36, No. 4, pp.1163-1166, 2000.

[17] D.-K. Hong, K.-C. Lee, B.-C. Woo, and D.-H. Koo, “Optimum design of electromagnet in magnetic levitation system for contactless delivery application using response surface methodology,” Proceedings of the 2008 International Conference on Electrical Machines, pp. 1-6, 2008.

[18] J.-M. Biedinger, and D. Lemoine, ”Shape sensitivity analysis of magnetic forces”, IEEE Trans.on Magn.,Vol.30, pp. 2309-2516, 1997.

[19] G. Sefkat, “The design optimization of the electromechanical actuator,” Structural and Multidisciplinary Optimization, February 2009, Volume 37, Issue 6, pp. 635–644, 2009.

[20] T.-W. Kim, and J.-H. Chang, “Optimal design of electromagnetic actuator with divided coil excitation to increase clamping force,” Journal of International Conference on Electrical Machines and Systems, pp. 1461-1464, 2014.

[21] K. Li, X. Zhang, and H. Chen, “Design Optimization of a Tubular Permanent Magnet Machine for Cryocoolers”, IEEE Transactions on Magnetics, Vol. 51, pp.1-8, 2015.

[22] A.-I. Dolan, “Optimization of DC electromagnet using design of experiments and FEM,” XIII-th IEEE International Conference on Applied and Theoretical Electricity – ICATE 2016, Craiova, Romania, October 06-08, pp. 1-6, 2016.

[23] A.-I. Dolan, “Three parameters optimization of acting force of DC electromagnet,” Proceedings of 11-th IEEE International Conference on Electromechanical and Power Systems – SIELMEN 2017, Iasi-Chisinau, October 11-13, pp. 1-4, 2017.

[24] G. Hortopan, Electrical apparatus of low voltage (in Romanian), Tehnica Publishing House, Bucharest, 1969.

[25] A.-I. Dolan, “Optimal Shape of DC Electromagnet,” Annals of the University of Craiova, Series: Electrical Engineering, Universitaria Publishing House, No. 41, pp. 9-13, 2017.

[26] A.-I. Dolan, “Improvement of Acting Force of DC Plunger-Type Electromagnet by Six Parameters optimization,” Proceedings of the XII-th International Conference on Electromechanical and Power Systems – SIELMEN 2019, October 9-11, pp. 1-5, Iasi-Chisinau, 2019.

[27] A.-I. Dolan, and F. Stefanescu, “Exhaustive optimization method based on DOE and FEM applied on a SMES device,” Proceedings of the XIX-th IEEE International Symposium on Electrical Apparatus and Technologies – SIELA 2016, Bourgas, Bulgaria, May 29-June 1, pp. 92-95, 2016.